Rarefaction Effects in Hypersonic Aerodynamics

Vladimir V. Riabov

Department of Mathematics and Computer Science, Rivier College, 420 S. Main St., Nashua, NH 03060, USA

Abstract. The Direct Simulation Monte-Carlo (DSMC) technique is used for numerical analysis of rarefied-gas hypersonic flows near a blunt plate, wedge, two side-by-side plates, disk, torus, and rotating cylinder. The role of various similarity parameters (Knudsen and Mach numbers, geometrical and temperature factors, specific heat ratios, and others) in aerodynamics of the probes is studied. Important kinetic effects that are specific for the transition flow regime have been found: non-monotonic lift and drag of plates, strong repulsive force between side-by-side plates and cylinders, dependence of drag on torus radii ratio, and the reverse Magnus effect on the lift of a rotating cylinder. The numerical results are in a good agreement with experimental data, which were obtained in a vacuum chamber at low and moderate Knudsen numbers from 0.01 to 10.

Keywords: DSMC method, aerodynamic coefficients, hypersonic flows, similarity parameters, torus, spinning cylinder
PACS: 47.11.Mn, 47.40.Ki, 47.45.Ab, 47.45.Dt, 47.85.Gj

INTRODUCTION

Stimulated by planetary exploration programs [1], numerical and experimental studies [1-8] of aerodynamics of simple-shape bodies have provided valuable information related to physics of rarefied-gas flows about spacecraft elements, testing devices, and in micro-channels. Numerous results were found in the cases of plates, wedges, cones, spheres, and cylinders [4-15].

In the present paper, hypersonic rarefied-gas flows about a plate, wedge, disk, two side-by-side cylinders and plates, torus, and spinning cylinder have been studied. The role of rarefaction parameter (Knudsen number), specific heat ratio, spinning rates, surface temperature, and geometrical factors is investigated. The DSMC method [2] and DS2G code [14] are used as a numerical technique for simulating low-density gas flows. Molecular collisions in air, nitrogen, carbon dioxide, helium, and argon are modeled using the variable hard sphere model [2]. The gas-surface interactions are assumed to be fully diffusive with full moment and energy accommodation. The validation [9] was tested in comparing numerical results with experimental data [6-8] related to the simple-shape probes.

AERODYNAMICS OF A BLUNT PLATE

The comparison of the DSMC recent numerical results for a drag coefficient of a parallel plate (thickness $\delta = 0.1L$) with experimental data [7] in air (specific heat ratio $\gamma = 1.4$) is studied for Knudsen numbers $Kn_{\infty,L}$ from 0.02 to 3.2, Mach number $M_\infty = 10$, and temperature factor $t_w = T_w/T_0 = 1$. Numerical results (see Fig. 1) correlate well with experimental data [7] at $0.02 < Kn_{\infty,L} < 1$. The free-molecular limit [3] is approached at $Kn_{\infty,L} > 3$.

The study of the influence of Mach number M_∞ on the aerodynamic characteristics of bodies of simple shape has been conducted at moderate values of the Knudsen number and at constant values of similarity parameters: $Kn_{\infty,\mathrm{L}}$, t_w, and γ. The regime of hypersonic stabilization [9] will occur at $M_\infty\theta >> 1$ in the case of streamlining of the thin bodies when the angle θ between the generatrix of the body surface and the direction of the upstream flow becomes small enough. This regime will be realized at smaller values of M_∞, if the angle θ increases.

The results of previous studies [6-8] indicate that the hypersonic flow independency principle [9] is realized in the transition rarefied-flow regime at $K = M_\infty \times \sin\theta > 1$. As was found in experiments [6-8], this principle is not true for thin bodies at small angles of attack in rarefied gas flows under the conditions $K < 1$.

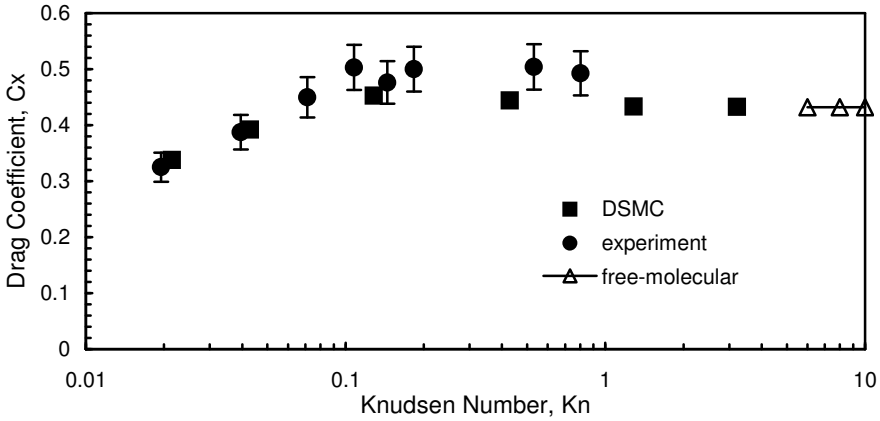

FIGURE 1. Drag coefficient of a plate vs. Knudsen number $Kn_{\infty,L}$ in air at $M_\infty = 10$ and $\alpha = 0$. Experimental data from Ref. 7.

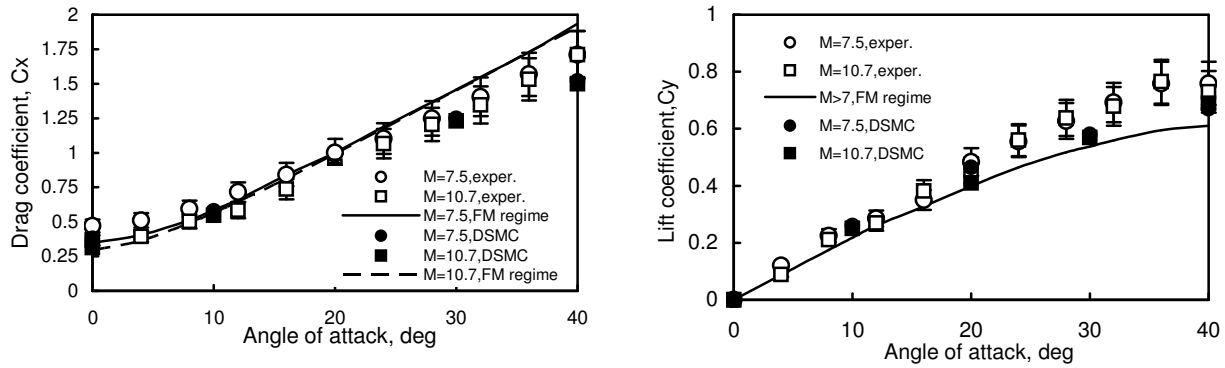

FIGURE 2. Drag and lift coefficients C_x, C_y for a blunt plate ($\delta = 0.06L$) at $Kn_{\infty,L} = 0.6$ and $M_\infty = 7.5$ (circles) and 10.7 (squares) in helium. Experimental data from Refs. 6-8.

The drag coefficient of a blunt plate having relative thickness $\delta = 0.06L$ becomes sensitive to the magnitude of the freestream Mach number in helium flow (Fig. 2, $M_\infty = 7.5$ and $M_\infty = 10.7$) at small angles of attack $\alpha < 12$ deg. The results calculated by the DSMC technique (filled markers) correlate well with the experimental data [6-8] (empty markers). For the lift coefficient, the free-molecular flow data [3], as well as computational and experimental results presented in Fig. 2, are independent of the Mach number, and the value $C_{y,FM}$ is less by approximately 15% than the value C_y for the transitional flow regime at $\alpha > 16$ deg. This phenomenon was discussed in Refs. 6-9.

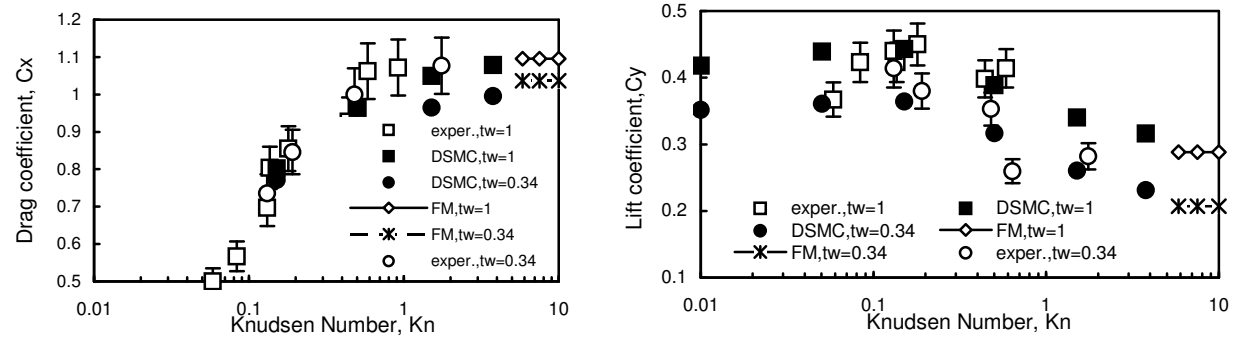

FIGURE 3. Drag and lift coefficients C_x, C_y for a blunt plate ($\delta = 0.1L$; $\alpha = 20$ deg) in air vs. Knudsen number $Kn_{\infty,L}$ at various temperature factors t_w. Experimental data from Ref. 7.

The temperature factor is other important similarity parameter [4-9], which effects pressure at the body surface. Numerical data for a plate ($\delta = 0.1L$) at angle attack $\alpha = 20$ deg and various $Kn_{\infty,L}$ has been studied (see Fig. 3). The lift coefficient, C_y changes non-monotonically from the continuum to the free-molecular flow regime. Maximum

values occur in the transition flow regime. The influence of t_w can be estimated as 25% for C_y. The results correlate well with the experimental data [7].

AERODYNAMICS OF A WEDGE

The dependence of drag and lift coefficients for a wedge (θ = 20 deg) on the angle of attack has been studied in numerical simulations of helium flow at $Kn_{\infty,L}$ = 0.3, t_w = 1, and the freestream Mach number M_∞ = 11.8. The DSMC results (squares) are shown in Fig. 4 for drag and lift coefficients. The base area of the wedge and its length were taken as the reference area and length.

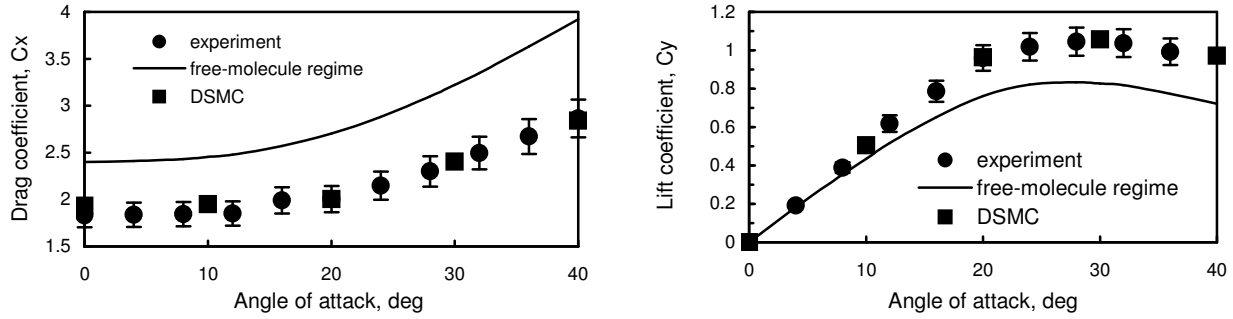

FIGURE 4. Drag and lift coefficients C_x, C_y for a wedge (θ = 20 deg) in helium flow at $Kn_{\infty,L}$ = 0.3 and M_∞ = 11.8. Experimental data from Refs. 6-9.

The numerical results correlate well with the experimental data [6-9] (circles), which were obtained in a vacuum wind tunnel at the same flow parameters. In both transitional and free-molecular [3] regimes, the characteristics are not sensitive to changes in upstream flow parameters at $M_\infty > 9$. Another interesting fact is that the lift-drag ratio in the transitional flow regime is larger by 50% than the corresponding parameter in the free-molecular regime [5-9].

AERODYNAMICS OF A DISK

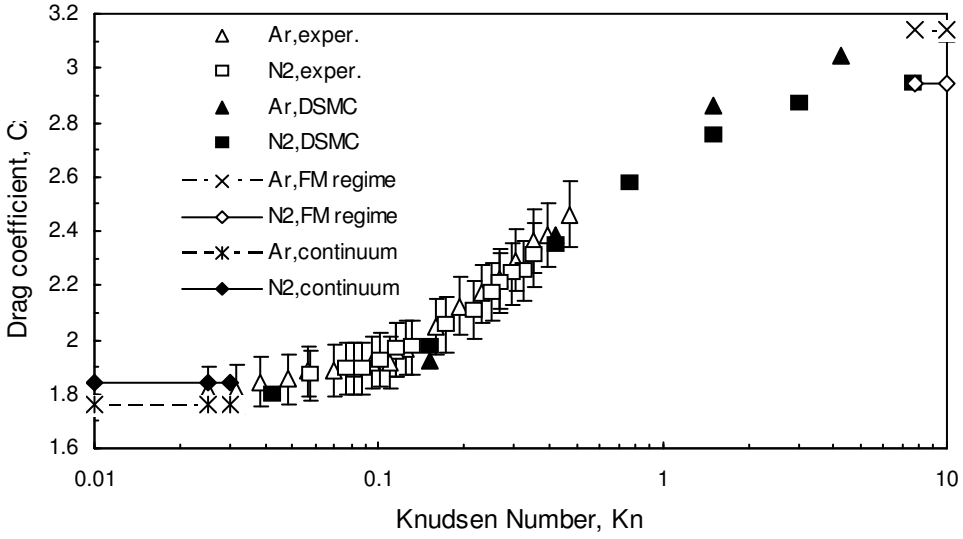

FIGURE 5. Drag coefficient C_x for a disk (α = 90 deg) vs. Knudsen number $Kn_{\infty,D}$ in argon and nitrogen. Experimental data from Refs. 6-8.

In the free-molecular flow regime, the influence of the specific heat ratio γ on the aerodynamic characteristics of bodies depends on the normal component of the momentum of the reflected molecules, which is a function of γ [7-9]. The same phenomenon can be observed at the transitional conditions in the case of the disk at $\alpha = 90$ deg. The nitrogen-argon pair was the most acceptable one for testing [6-9]. The dependencies of C_x of the disc for Ar (filled triangles) and N_2 (filled squares) are shown in Fig. 5 for a wide range of Knudsen numbers ($Kn_{\infty,D}$). At the same parameters of the upstream flow, numerical data obtained by the DSMC technique for different models of molecules are compared with experimental data [6-8]. This analysis could be applied to the design of a disk ballute [16].

The influence of specific heat ratio on the drag coefficient is more significant for large values of $Kn_{\infty,D} > 1$. In the free molecular regime ($Kn_{\infty,D} > 7$) an increase of C_x is observed as γ increases [3, 9]. This increase is caused by the dependence on γ of the reflected momentum of the molecules at $t_w = 1$. The degree of this influence has been evaluated as 8% at $Kn_{\infty,D} > 2$. As the number $Kn_{\infty,D}$ decreases, this influence decreases, and at $Kn_{\infty,D} < 0.4$, the drag coefficient of the disk in diatomic gas becomes larger than that for a monatomic gas. In the continuum flow regime, the dependence of the drag-coefficient on γ difference is insignificant.

AERODYNAMICS OF TWO SIDE-BY-SIDE PLATES

The flow pattern over two side-by-side plates is sensitive to the geometrical parameter, H/L, where $2H$ is a distance between the plates. The influence of this parameter on the flow structure has been studied for hypersonic flow of argon at $M_\infty = 10$, $t_w = 1$, and $0.024 \le Kn_{\infty,L} \le 1.8$. At $H \le 0.5L$, the flow area between two side-by-side plates becomes subsonic [10]. At $H > 0.5L$, two oblique shock waves interact in the vicinity of the symmetry plane generating the normal shock wave and the Mach reflected waves far behind the bodies [10].

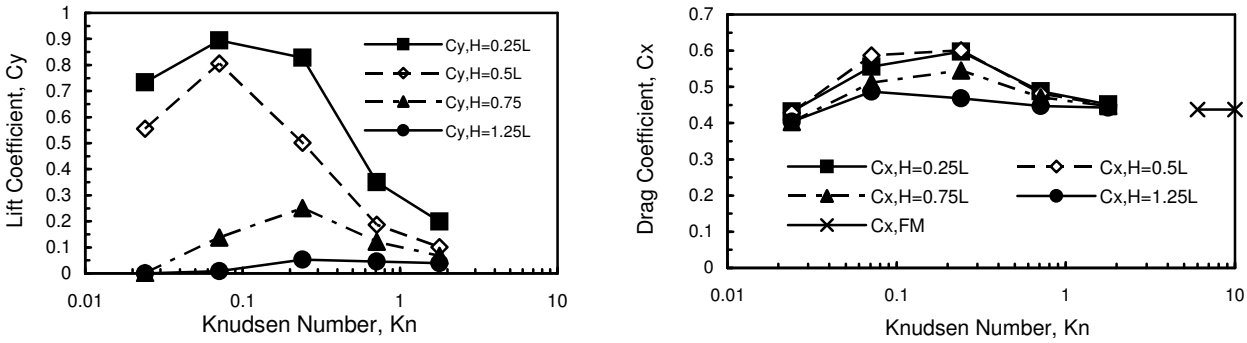

FIGURE 6. Lift and drag coefficients C_y, C_x of the side-by-side plates vs. Knudsen Number $Kn_{\infty L}$ at $M_\infty = 10$.

Numerical results for the total lift and drag coefficients are also studied (see Fig. 6). The repulsive lift force becomes significant at $H/L \le 0.75$, with the average lift-drag ratio of 1.6 for plates in the transition regime [10]. The rarefaction effects are responsible for non-monotonic dependency of the lift on the Knudsen number at $1.25 \ge H/L \ge 0.25$ (Fig. 6). The drag coefficient (Fig. 6) increases with Knudsen number, reaches a maximum, and then decreases to the free-molecular value [3]. The geometrical factor becomes insignificant as to its influence on the drag as both the continuum and free-molecule flow regimes are approached.

AERODYNAMICS OF A TORUS

Strong influences of the geometrical factor, H/R (ratio of the distance between the axis of symmetry and the torus disk center H, and the torus cross-section radius R) and the Knudsen number, $Kn_{\infty,R}$ on the flow structure near a torus (the shape of shock waves and the stagnation point location), skin friction, pressure distribution, and drag have been found. The influence of these parameters on the flow structure has been studied in argon, nitrogen, and carbon dioxide at $M_\infty = 10$, $2R \le H \le 8R$, and $0.0167 \le Kn_{\infty,R} \le 10$.

At values of the parameter $H/R > 6$, the conical shock waves interact in the vicinity of the flow symmetry axis far beyond the torus throat, creating the Mach disk. The reflected conical wave has a different pattern of the interaction with the supersonic flow behind a torus in continuum and rarefied flow regimes [11]. At $H/R \ge 8$, the flow near a torus is similar to that one about two side-by-side cylinders [15].

At smaller values of the parameter $H/R \leq 4$, the shape of a front shock wave becomes normal, and the subsonic area is restricted by the location of the shock wave and the torus throat [11]. This "chocked-flow" effect plays a fundamental role in the redistribution of pressure and skin friction along the torus surface. The location of the stagnation-point ring (estimated through distributions of pressure and skin-friction coefficients) is moving from the front area to the torus throat after reducing the outer torus radius, H.

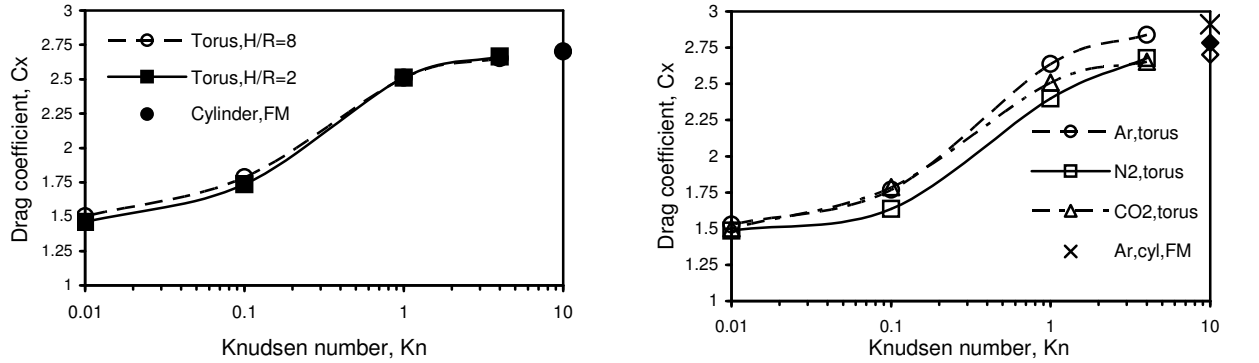

(a) Drag coefficient C_x of a torus in carbon dioxide **(b) Drag coefficient C_x of a torus ($H/R \geq 6$) in Ar, N_2, and CO_2**

FIGURE 7. Drag coefficient C_x of a torus vs. Knudsen number $Kn_{\infty,D}$ in argon, nitrogen, and carbon dioxide at $M_\infty = 10$.

Numerical results of the total drag coefficient of a torus are also studied (see Fig. 7). The drag coefficient increases with increasing the Knudsen number. The geometrical factor becomes insignificant on the drag at $H/R \geq 6$ under continuum and free-molecule flow regimes. Heat transfer on toroidal baluttes was studied in Refs. 1, 16-18.

AERODYNAMICS OF A ROTATING CYLINDER

At subsonic flow conditions, the speed ratio $S = M_\infty \cdot (0.5 \cdot \gamma)^{1/2}$ becomes small, and aerodynamic coefficients of a rotating cylinder become sensitive to the ratio magnitude [3, 13, 19]. The transition flow regime has been studied in argon at $M_\infty = 0.15$ and spin ratio $W = \Omega D/2U_\infty = 1$, 3, and 6. The lift and drag coefficients are shown in Fig. 8.

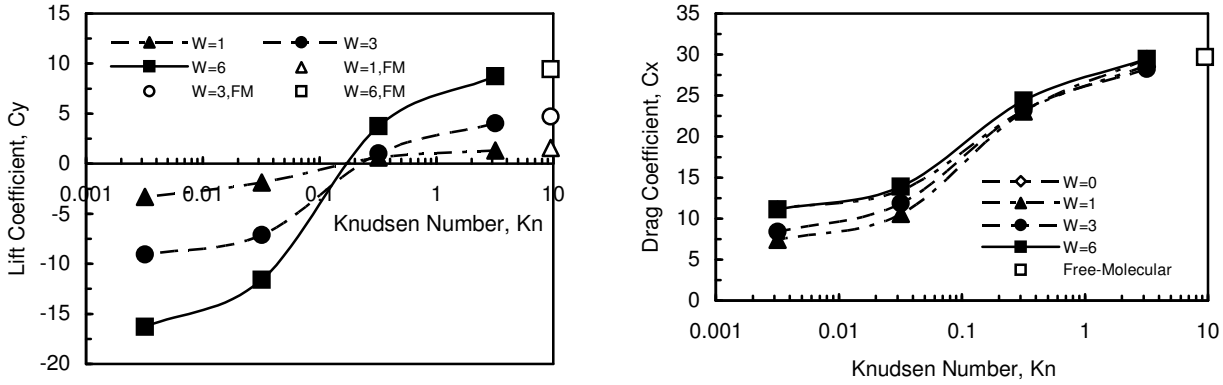

FIGURE 8. Lift and drag coefficients C_y, C_x of a spinning cylinder vs. Knudsen number $Kn_{\infty,D}$ at $M_\infty = 0.15$ and different spin rates W in argon.

In the transition flow regime ($Kn_{\infty,D} > 0.03$), both the incident and reflected molecules significantly influence the lift [13]. The incident molecules dominate when $Kn_{\infty,D} < 0.1$, and the reflected molecules dominate when $Kn_{\infty,D} > 0.1$. The lift changes sign for the cylinder spinning in counter-clockwise direction. The drag becomes a slow function of the spin rate. In the near-free-molecule flow regime ($Kn_{\infty,D} = 3.18$), the asymmetry of the flow in upper and bottom regions is significant [13]. The flow disturbances are concentrated in the vicinity of the spinning surface. In the near-continuum flow regime ($Kn_{\infty,D} = 0.032$), the circulating zone is much wider. These flow-pattern differences dominate the character of molecule-surface interactions.

At supersonic flow conditions, the speed ratio S becomes large, and the aerodynamic coefficients become less sensitive to its magnitude [13, 19]. In the present study, the transition flow regime has been investigated numerically at $M_\infty = 10$, $\gamma = 5/3$ (argon gas), and spin ratio $W = 0.03$ and $W = 0.1$.

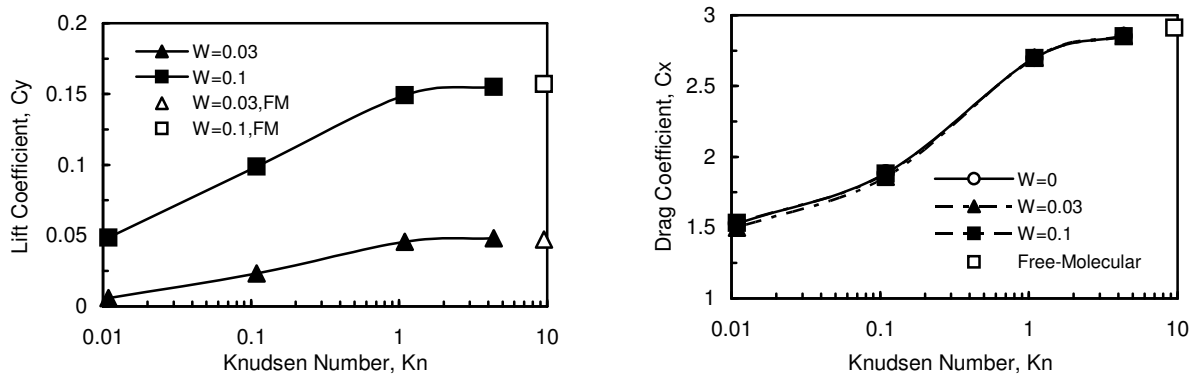

FIGURE 9. Lift and drag coefficients C_y, C_x of a spinning cylinder vs. Knudsen number $Kn_{\infty,D}$ at $M_\infty = 10$ and different spin rates W in argon.

The lift and drag coefficients are shown in Fig. 9. For the lift coefficient, the influence of reflected molecules is dominant in the transition-flow regime ($Kn_{\infty,D} > 0.03$). The incident-molecule input becomes significant at Knudsen number $Kn_{\infty,D} < 0.1$ [13]. Under the considered flow conditions, the lift coefficient has a positive sign (which is opposite to the sign under the continuum flow regime) for the cylinder spinning in a counter-clockwise direction. The drag coefficient is insensitive to the spin rate. The values of C_y and C_x at $Kn_{\infty,D} > 4$ are near the magnitudes of the coefficients for the free-molecule flow [3, 19].

The flow characteristics are different in these cases [13]. For a small spin rate, $W = 0.1$, the zone of circulating flow is located in the vicinity of the surface, and it does not affect the flow zone located far from the surface. The flow pattern becomes asymmetrical. The differences in flow patterns dominate the character of molecule-surface interactions, and they characterize the differences in the performance parameters under significantly distinct flow conditions [13]. Similar effects for a spinning sphere were studied in Refs. 20 and 21.

REFERENCES

1. Gnoffo, P., *J. Spacecraft and Rockets* **40** (3), 305-312 (2003).
2. Bird, G. A., *Molecular Gas Dynamics and the Direct Simulation of Gas Flows*, 1st ed., Oxford University Press, Oxford, England, UK, 1994, pp. 340-377.
3. Kogan, M. N., *Rarefied Gas Dynamics*, Plenum Press, New York, 1969, pp. 345-390.
4. Koppenwallner, G., and Legge, H., "Drag of Bodies in Rarefied Hypersonic Flow" in *Thermophysical Aspects of Re-Entry Flows*, edited by J. N. Moss and C. D. Scott, AIAA, Washington, DC, 1994, pp. 44-59.
5. Gusev, V. N., Kogan, M. N., and Perepukhov, V. A., *Uchenyye Zapiski TsAGI* **1** (1), 24-31 (1970) (in Russian).
6. Gusev, V. N., Klimova, T. V., and Riabov, V. V., *Uchenyye Zapiski TsAGI*, **7** (3), 47-57 (1976) (in Russian).
7. Gusev, V. N., Erofeev, A. I., Klimova, T. V., Perepukhov, V. A., Riabov, V. V., and Tolstykh A. I., *Trudy TsAGI* **1855**, 3-43 (1977) (in Russian).
8. Riabov, V. V., *J. Aircraft* **32** (3), 471-479 (1995).
9. Riabov, V. V., *J. Spacecraft and Rockets* **35** (4), 424-433 (1998).
10. Riabov, V. V., *J. Spacecraft and Rockets* **39** (6), 910-916 (2002).
11. Riabov, V. V., *J. Spacecraft and Rockets* **36** (2), 293-296 (1999).
12. Riabov, V. V., *J. Spacecraft and Rockets* **41** (4), 698-703 (2004).
13. Riabov, V. V., *J. Spacecraft and Rockets* **36** (3), 486-488 (1999).
14. Bird, G. A., "The DS2G program User's Guide. Version 3.2," G. A. B. Consulting Pty, Killara, Australia, 1999, pp. 1-56.
15. Riabov, V. V., AIAA Paper 2002-3297 (2002).
16. McRonald, A., AIAA Paper 99-0422 (1999).
17. Hall, J., and Le, A., *AAS/AIAA Space Flight Mechanics Meeting*, AAS Paper 01-235 (2001).
18. Moss, J. N., *J. Spacecraft and Rockets* **44** (2), 289-298 (2007).
19. Ivanov, S., and Yanshin, A., *Fluid Dynamics* **15** (3), 449-453 (1980).
20. Borg, K. I., and Söderholm, L. H., *European J. of Mechanics - B/Fluids* **27** (5), 623-631 (2008).
21. Volkov, A. N., *Fluid Dynamics* **44** (1), 141-157 (2009).